Polymer Chemistry

ROYAL SOCIETY OF CHEMISTRY

PAPER

View Article Online
View Journal

Cite this: DOI: 10.1039/d1py00250c

Facile synthesis of GalNAc monomers and block polycations for hepatocyte gene delivery†

Matthew R. Bockman, Rishad J. Dalal, Ramya Kumar and Theresa M. Reineke *

Received 23rd February 2021,
Accepted 16th June 2021

DOI: 10.1039/d1py00250c

rsc.li/polymers

The ability to design liver-targeted polymers for nucleic acid delivery vehicles is plagued with difficulties ranging from polymer-mediated cellular toxicity to challenges in synthesizing monomers that enable facile cell-specific polymeric gene delivery vehicles. Herein is presented an improved synthetic route to a *N*-acetyl-D-galactosamine (GalNAc)-derived monomer (two steps, 91% overall yield) and its incorporation into a library of nine diblock co-polymers with 2-aminoethylmethacrylamide (AEMA) and two end-group functionalized AEMA homopolymers. These polymers were complexed with plasmid DNA (pDNA) into polyplexes and evaluated for the toxicity, uptake and transfection efficiency against cultured hepatocytes (HepG2) at N/P ratios of 2.5, 5, and 10. All polyplexes showed a range of cell survivability between 60–90%, an improvement over JetPEI, a commercial transfection reagent, when dosed at standard concentrations. Although GalNAc block length does not play a significant role in cellular uptake of Cy-5 labeled pDNA, it has a heavy influence on the transfection efficiency of luciferase-encoded pDNA where longer GalNAc block lengths give rise to higher transfection efficiencies. Overall, this work demonstrates a greatly improved route to GalNAc monomer synthesis, which that can be incorporated into polymers that target hepatocytes.

Introduction

After nearly three decades of research, gene therapy has become one of the most promising therapies available for a variety of applications such as neurodegenerative,[1] immunodeficiency,[2] and cardiovascular[3] disorders as well as various forms of cancer.[4] While viral gene therapy has remained an attractive area of research due to the high efficiency of transgene delivery, several problematic factors still plague this delivery paradigm including: the immunogenicity of these delivery vehicles, non-specific transgene delivery, genetic cargo capacity, and substantial financial burdens in large-scale production of treatments.[5,6] These factors prompt development of non-viral strategies to circumvent the multiple obstacles that viral systems possess. Among several non-viral systems are cationic polymers, which can provide affordable, safe and versatile delivery methods.[7] Cationic polymers such as polyethyleneimine (PEI),[8] poly((2-dimethylamino) ethyl methacrylate) (PDMAEMA),[9] and poly(2-aminoethylmethacrylamide) (PAEMA)[10,11] readily condense the anionic phosphate backbone of DNA forming nanoparticles known as polyplexes.[12] These are then readily internalized into cells through either caveolae or clathrin-mediated endocytosis.[13,14] The low cost, high degree of characterization and optimization makes these polymers an attractive option for non-viral delivery systems. However, most of these polymers are derived from commercially available or readily accessible monomers, which can severely limit the chemical diversity, functionality, performance, and specificity of polymer vehicles. One route to approach this problem is by creatively designing and synthesizing new functional monomers. However, enthusiasm to utilize synthetic monomers is often abated when multi-step synthesis schemes are necessary to make the structures and the associated difficulty in obtaining pure quantities necessary for polymer synthesis.

Design of delivery vehicles that promote specificity in targeting tissue types is of high interest to this field. Targeting cells of hepatic origin are important for several gene therapy applications related to enzyme replacement therapies and liver diseases. Indeed, the liver is responsible for expressing and excreting serum proteins into the blood, which is a mechanism that can be utilized for prolonged therapeutic intervention to replace direct protein therapy administration. This approach is of high interest as a treatment for inherited or acquired disorders (*e.g.* acute intermittent porphyria, α1-antitrypsin deficiency, ornithine transcarbamylase deficiency, hyperbilirubinemia, hemophilia A/B, Wilson's disease, cirrho-

Department of Chemistry, University of Minnesota, Minneapolis, MN 55455, USA. E-mail: treineke@umn.edu; Tel: +(612) 624-8042

†Electronic supplementary information (ESI) available: Detailed experimental procedures and characterization of all synthesized monomers, CTAs and polymers described; ^{1}H NMR spectra of all polymers; cytotoxicity, transfection and Cy5 internalization assay experimental procedures. See DOI: 10.1039/d1py00250c

sis, hepatic tumors, hepatitis B/C).[15,16] Receptor-mediated targeting is a common strategy to deliver polyplexes to specific cell types, and of particular importance are ligands targeting the liver.[17] To that end, the binding of *N*-acetyl-D-galactosamine (GalNAc) to the asialoglycoprotein receptor (ASGPR) on hepatocytes has been studied extensively in the development of structures to deliver genetic material such as DNA and siRNA (Fig. 1).[10,18–22] Triantennary structures have been shown to possess over one thousand times higher affinities for ASGPRs than their monovalent counterparts as measured by improved inhibitory concentrations (IC_{50}) as well as shown to exhibit *in vivo* liver targeting capabilities.[23,24] However, their lack of widespread use in the field can be attributed to the high cost of reagents, synthetic difficulty (*i.e.* over six synthetic/purification steps), and subsequent low yields.[23,25–29]

By increasing the valency of ligands on the polymers that complex genetic payloads into polyplexes, the binding efficiency to the receptor should increase. This can be accomplished by synthesizing polymers possessing GalNAc binding moieties *in lieu* of analogous triantennary architectures. Previous work has studied statistically-incorporated galactosylated glycopolymers that were able to successfully transfect hepatocytes *via* ASGPR binding.[30] Prior work from our lab has also shown that by incorporating each functional monomer into blocks greatly improves pDNA binding and transfection efficiency compared to their statistically incorporated counterparts.[31,32] Additionally, we previously presented the successful synthesis of block polymers that display GalNAc in a multivalent manner, bind to ASGPR on cultured cells, and promote selective gene transfection in a hepatocyte cell models (HepG2).[10] These polymers were composed of a methacrylamide-functionalized GalNAc (MAGalNAc, **3**) block of fixed length (n = 62) and a cationic 2-aminoethylmethacrylamide (AEMA) block of varying lengths (n = 19, 33 and 80). Although we were able to show both *in vitro* and *in vivo* efficacy of these polymers for liver targeting, only three GalNAc-derived polymers – containing AEMA block lengths of 19, 33, and 80 – were explored. This work also showed evidence of receptor-mediated uptake *via* a competitive inhibitory assay wherein uptake of Cy5-labeled asialofetuin (ASF-Cy5, a known glycoprotein ligand for ASGPR) was measured in the presence and absence of poly(MAGalNAc)$_{62}$, GalNAc, Galactose, glucose and a polymer derived from a glucose-based monomer. The poly(MAGalNAc)$_{62}$ was shown to inhibit the uptake of this ligand, compared to monomeric GalNAc. However, a significant bottleneck for that work (and synthesizing more polymer variants) was primarily due to the difficulty in obtaining monomer **3**, obtained in four steps – most of which require purification that limits the overall yield.[10] While successful for the purpose of that work, the difficulty for scaling this route limits **3** as a useful monomer for studies with polymers used for GalNAc/ASGPR binding. Thus, a new route to **3** is necessary to enable facile production of block polymers containing GalNAc and presented below.

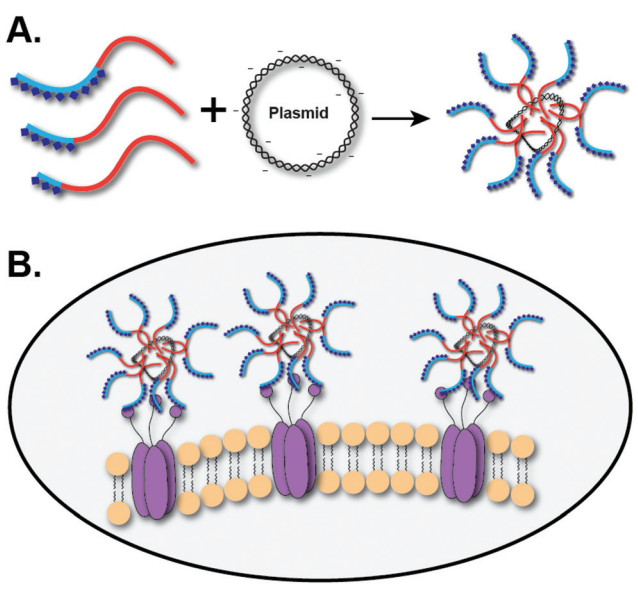

Fig. 1 (A) Schematic of polymer library and polyplex formation wherein the cationic polymer block (shown in red) binds to the anionic backbone of plasmid DNA (pDNA). (B) The exposed multivalent GalNAc ligand block (shown in blue) of the polyplex binds to the ASGPRs on the surface of hepatocytes, promoting targeting and internalization of polyplexes.

Results and discussion

Inspired by the success of those GalNAc-containing polymers and the desire to continue our efforts in expanding our GalNAc-containing polymer library, we sought to improve upon the synthesis and yield of monomer **3** amenable to scaleup. Herein, we describe a substantially improved route to **3** in only two steps with 91% overall yield that can effectively produce the monomer at scale for rapid polymer synthesis. To investigate how the GalNAc block length affects hepatocyte gene delivery, we then synthesized a library of poly(MAGalNAc-*b*-AEMA) (**PGxAy**) diblock copolymers with varying **3** and AEMA lengths. To both examine the effects of a telechelic functionalized polymer on gene delivery efficiency and expand the structural diversity of our library, an additional end-group GalNAc-functionalized chain-transfer agent (CTA) was synthesized *via* copper-catalyzed azide–alkyne cycloaddition (CuAAC) and polymerized with AEMA (termed PAEMA-Gal). The greatly improved synthetic route to monomer **3**, and the subsequent synthesis and physiochemical characterization of a poly(MAGalNAc-*b*-AEMA) and PAEMA-Gal family of polymers is described. We also examined the cytotoxicity and efficacy toward transfecting cultured hepatocellular carcinoma (HepG2) cells for each polymer variant. Combined with our previous work, this suite of polymers further shows promise of using GalNAc block polymers in formulations to deliver nucleic acids to hepatocytes. Moreover, the new, efficient, and robust synthetic route to the GalNAc monomer **3** to create block polymers and the monofunctionalized GalNAc chain transfer agent can be useful to the field for pioneering novel

GalNAc-containing polymers for numerous nonviral gene delivery applications.

Based on the success of our previous work,[10] we decided to utilize the same GalNAc-based monomer previously synthesized. However, the reported synthesis consisted of four discrete steps with moderate yields and multiple rounds of purification, leading to difficulty in largescale multi-gram production of this monomer. Starting with commercially available 2-acetamido-1,3,4,6-tetra-*O*-acetyl-2-deoxy-β-D-galactopyranose (**1**), the conversion of **1** to the corresponding intermittent oxazoline *via* trimethylsilyl trifluoromethanesulfonate (TMSOTf) in 1,2-dichloroethane (DCE) at a slightly elevated temperature (50 °C), directly followed by nucleophilic addition of *N*-(2-hydroxyethyl)methacrylamide in the same pot afforded the peracetylated methacrylamide monomer **2** in high yields (97%) after purification (Scheme 1). This is a significant improvement over the previously reported route, which started with acetylation of *N*-acetylgalactosamine, oxazoline formation, and nucleophilic substitution with *N*-(2-hydroxyethyl)methacrylamide in three discrete steps and a 46% overall yield.[10] The ability to eliminate two steps and a round of purification greatly eases the synthetic burden for potential scale up. Subsequent methanolysis of the *O*-acetyl groups using sodium methoxide afforded the final MAGalNAc monomer **3**, which can be isolated after workup without the need for any further purification (Scheme 1). This two-step route afforded the monomer more efficiently and consistently as well as enabled rapid multi-gram production compared to previously reported routes.[10,18]

Monomer **3** was then subjected to reversible addition–fragmentation chain transfer (RAFT) polymerization conditions using 4-cyano-4-(propylsulfanylthiocarbonyl) sulfanylpentanoic acid (CPP)[33] as the CTA and 4,4′-azobis(4-cyanopentanoic acid) (V-501) as the initiator in 2 : 1 water/ethanol mixture to afford the corresponding poly(MAGalNAc) polymers (**PGx**, where *x* is the degree of polymerization for the MAGalNAc block; Scheme 1). This method was slightly altered from previous reports and gave more consistent results when synthesizing **PGx** polymers.[10,18] Interestingly, the longer MAGalNAc block lengths required much longer reaction times and a higher monomer feed to obtain the desired length; we were thus unable to obtain polymers with MAGalNAc block lengths much greater than previously reported with the longest polymer having a GalNAc block length of 102. The macroCTA **PGx** library was then chain-extended with AEMA to give the library of diblock copolymers as previously described (**PGxAy**, where *y* is the degree of polymerization for the AEMA block; Scheme 1, Table 1, Fig. 2).[10]

Concurrent to our work synthesizing the diblock polymers, a monovalent GalNAc-functionalized polymer was also created

Table 1 Molecular weight, dispersity, and degree of polymerization (DP) of the polymer library

Polymer (**PGxAy**)[a]	M_n[a] (kDa)	$Đ$[a]	MAGalNAc DP (x)[a]	AEMA DP (y)[a]
PG26A30	13.9	1.11	26	30
PG26A41	15.4	1.18	26	41
PG31A55	19.5	1.32	31	55
PG31A76	23.1	1.35	31	76
PG40A54	22.5	1.45	40	54
PG62A19[b]	23.0[b]	1.29[b]	62	19
PG62A33[b]	25.0[b]	1.32[b]	62	33
PG102A12	36.3	1.22	102	12
PG102A60	44.2	1.23	102	60
PAEMA$_{74}$	12.7	1.38	N/A	74
PAEMA$_{96}$-Gal	16.8	1.34	N/A	96

[a] Number-average molecular weight (M_n) in kilodaltons (kDa) and dispersity ($Đ$), as determined by SEC using an aqueous eluent of 0.1 M Na_2SO_4 in 1 wt% acetic acid at a flow rate of 0.3 mL min^{-1} on Eprogen columns [CATSEC1000 (7 μm, 50 × 4.6), CATSEC100 (5 μm, 250 × 4.6), CATSEC300 (5 μm, 250 × 4.6), and CATSEC1000 (7 μm, 250 × 4.6)] with a Wyatt HELEOS II static light scattering detector (λ = 662 nm) and an Optilab rEX refractometer (λ = 658 nm). [b] The synthesis and characterization of **PG62A19** and **PG62A33** has been reported previously.[10]

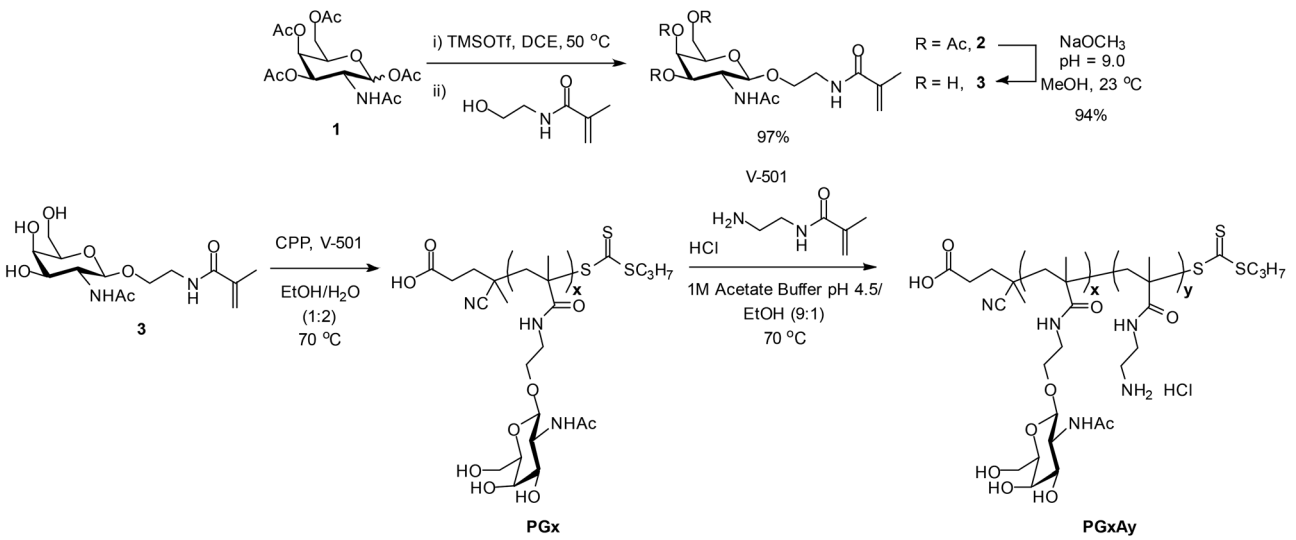

Scheme 1 Improved synthetic route of MAGalNAc monomer (**3**) and GalNAc-based diblock copolymers (**PGxAy**).

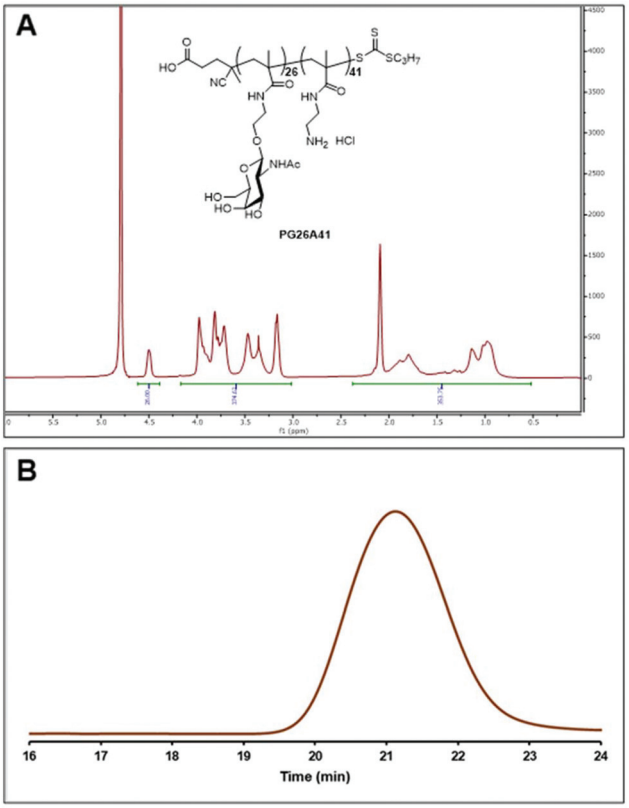

Fig. 2 Representative characterization of synthesized polymer **PG26A41** showing (A) ^{1}H NMR in D_2O and (B) SEC traces.

as a control to probe the transfection efficiency of the subsequent monovalent polyplex. To accomplish this, we synthesized an azido-modified 4-cyano-4-(dodecylsulfanylthiocarbonyl) sulfanylpentanoic acid (CDP) CTA with an alkyne-substituted GalNAc (**5**) to afford a GalNAc-conjugated CTA (**9**), for use in RAFT polymerization reactions. Briefly, **1** was treated with TMSOTf followed by alkyne **4** to afford the acetylated glycoside alkyne **5** and subsequent base-promoted methanolysis furnished alkynylated GalNAc **6** (Scheme 2). Steglich esterification of CDP (**7**) with an azido-functionalized tri(ethyleneoxide) gave rise to a novel azido-CTA **8.** Interestingly, although azide-functionalized CTAs have been synthesized previously,[34] and a few are available commercially such as 3-azidopropyl 2-{[(dodecylthio) carbonyl]thio}-2-methylpropanoate, there is a distinctive lack of azide-functionalized CTAs derived from **7**, and only one example was found with a related CTA synthesized in a 2019 patent.[35] Finally, a copper-catalyzed azide–alkyne cycloaddition (CuAAC) with moderate heating (40 °C) afforded fully functionalized CTA **9** (termed CDP-Gal) in moderate yield (Scheme 2). This chemistry also provides a foundation for conjugating other alkynylated functionalities onto **8** *via* CuAAC to functionalize polymers with targeting end groups. RAFT polymerization of AEMA using both **7** or **9** as the CTA in 9 : 1 1 M aqueous acetate buffer (pH 4.5)/ethanol afforded the cationic $PAEMA_{74}$ or monovalent GalNAc functionalized $PAEMA_{96}$ ($PAEMA_{96}$-Gal) polymers, respectively (Scheme 3) that varied in length.

In addition to the improved synthetic methods, we sought to investigate how each block length and the ratio of the two block lengths affect toxicity and delivery efficiency to hepatocytes. Thus, we characterized our polymer block lengths as "short" (between 19 and 33 repeat units), "medium" (between 41 and 62 repeat units) and "long" (over 70 repeat units) and our library reflects the various iterations of each block length (Table 1). The family of 11 polymers was characterized by size-exclusion chromatography (SEC) to determine their number-average molecular weights and dispersities (Table 1). ^{1}H NMR was used to confirm the molecular weights of the polymers by direct comparison of the MAGalNAc block to the AEMA block for the diblock polymers. The molecular weight of $PAEMA_{96}$-Gal was verified by ^{1}H NMR by comparison of the AEMA peaks to the GalNAc end-group peaks. The dispersities are consistent with previously synthesized MAGalNAc diblock polymers.[10] The number-average value was used to determine the degree of polymerization.

These polymers were then evaluated for their ability to successfully complex with plasmid DNA (pDNA). The ratio of each polyplex formulation to pDNA is determined by the N/P ratio, or the ratio of ionizable amines (cationic block, N) to the negatively charged phosphates (P) on the DNA backbone. Polyplexes were formed by mixing differing concentrations of polymers to an equal volume of pDNA (50 ng μL^{-1}) and analyzing after incubation at 23 °C for 1 h. Consistent with MAGalNAc-containing polyplexes previously synthesized,[10] all polymers from the library bound to pDNA as evident by the hinderance of pDNA migration on agarose gel at N/P ratios of 2.5, 5, and 10 (Fig. S4†). Additionally, dynamic light scattering (DLS) was used to determine polyplex size and colloidal stability (Fig. 3, Table S2†). Polyplexes were formed as described above at the same N/P ratios, diluted with reduced-serum OptiMEM, and measured for their hydrodynamic radii immediately, 1, 2, and 4 h after dilution. All diblock polymers had hydrodynamic radii ranging from 31 to 142 nm, with the length of MAGalNAc block potentially playing no significant role that affects these values, as well as no evidence suggesting aggregation had occurred after 4 h; the exception is **PG102A60**, where at N/P 2.5 the polyplex is much greater than the rest of the library (Fig. 3). The lack of aggregation can be attributed to the hydrophilic nature of the MAGalNAc block and thus impart colloidal stability to the polyplexes. Conversely, the PAEMA polymers were much larger, ranging from 200 to 870 nm, and seemed to aggregate at longer incubation times, owing to the benefit of a GalNAc block for polyplex stability (Table S5†).

HepG2 cell viability was determined after transfection using a CCK-8 cell counting kit (Fig. 4). Generally, all polyplexes showed the trend of decreased cell viability as the N/P ratio increased, with a N/P ratio of 10 being the most toxic for most polyplexes (Table S6†). At N/P ratios of 2.5 and 5, all polyplexes showed a range of cell survivability between 60–90%. Interestingly, appending a single GalNAc onto PAEMA did not show a significant difference in toxicity towards HepG2 cells, perhaps owing to the overall miniscule change in structure between the functionalized $PAEMA_{96}$-Gal and unfunctionalized

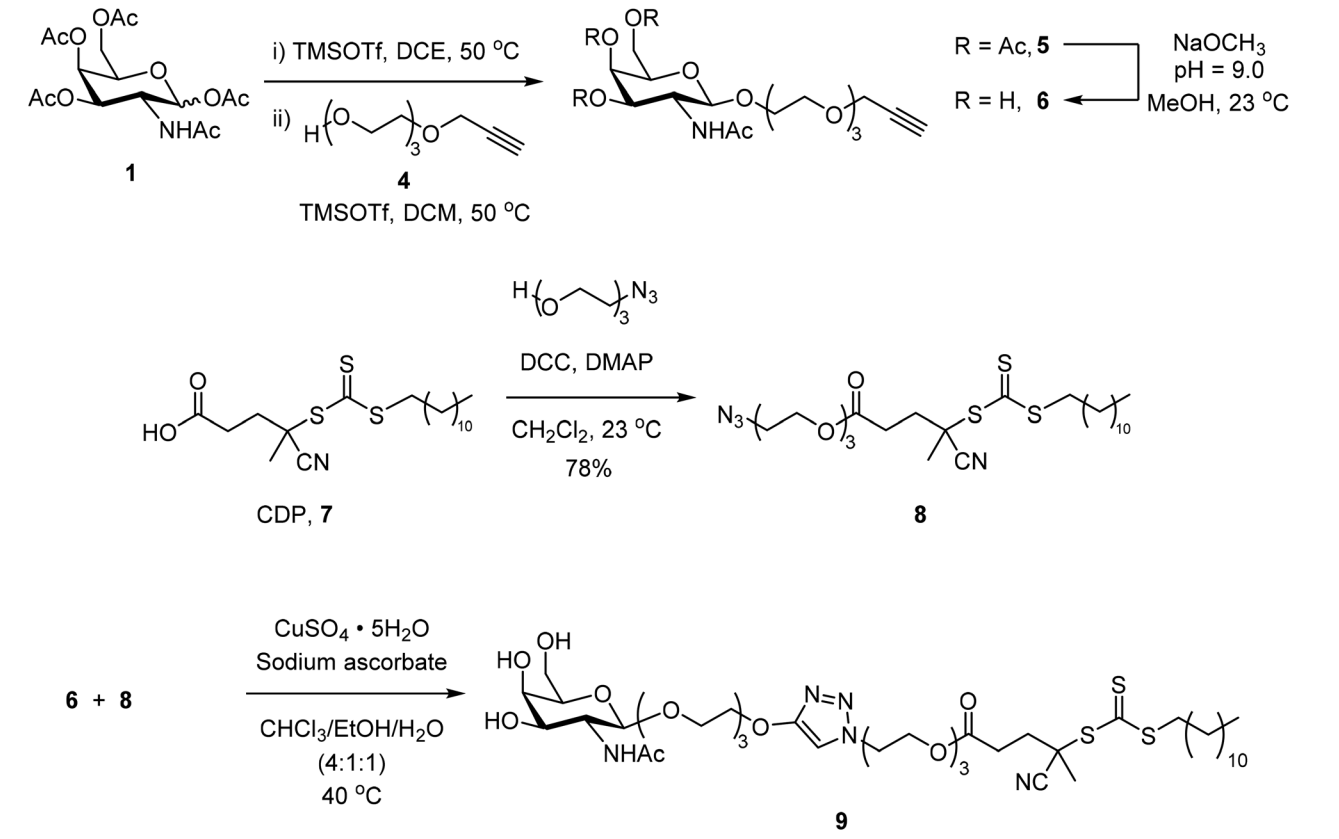

Scheme 2 Synthesis of monovalent GalNAc CTA (**8**).

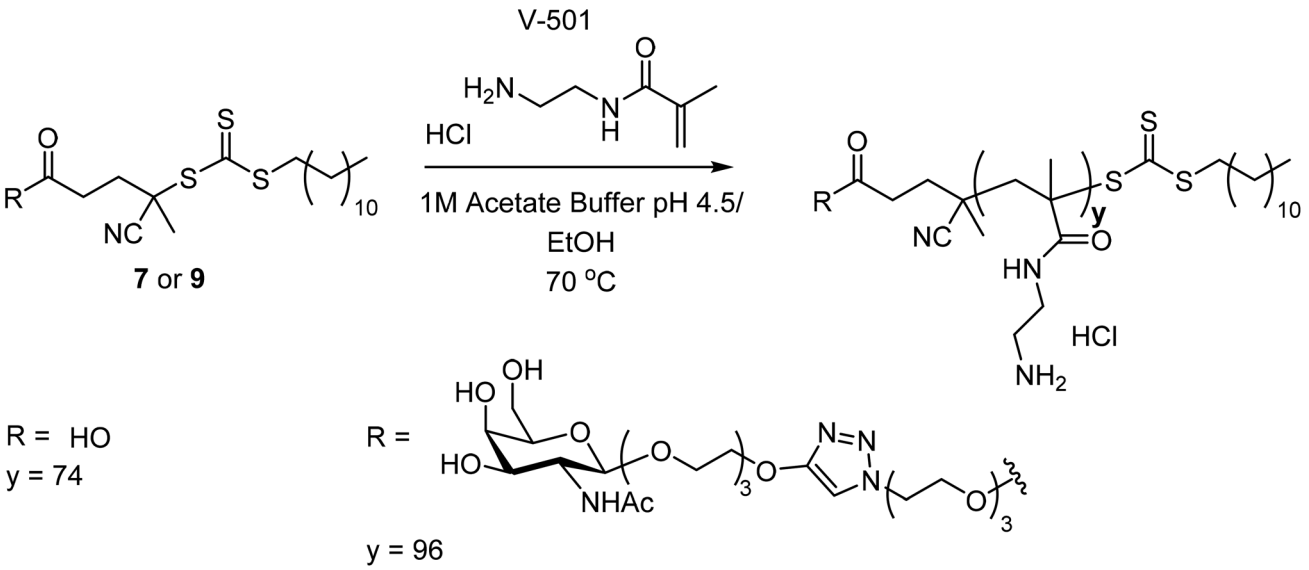

Scheme 3 RAFT polymerization of AEMA using CDP (**7**) or CDP-Gal (**9**).

$PAEMA_{74}$. All polyplexes – except **PG62A19** – were less toxic than the commercially available JetPEI, which has a well-known toxicological profile. There was otherwise no other reconcilable pattern able to be discerned between MAGalNAc or AEMA length and cell viability.

The binding of the multivalent GalNAc to the ASGPRs on the surface of hepatocytes promotes cell-specific recognition and internalization of the polyplexes *via* receptor-mediated endocytosis.[10,18] To verify cellular internalization of our polyplexes, we transfected HepG2 cells with pDNA labeled with a

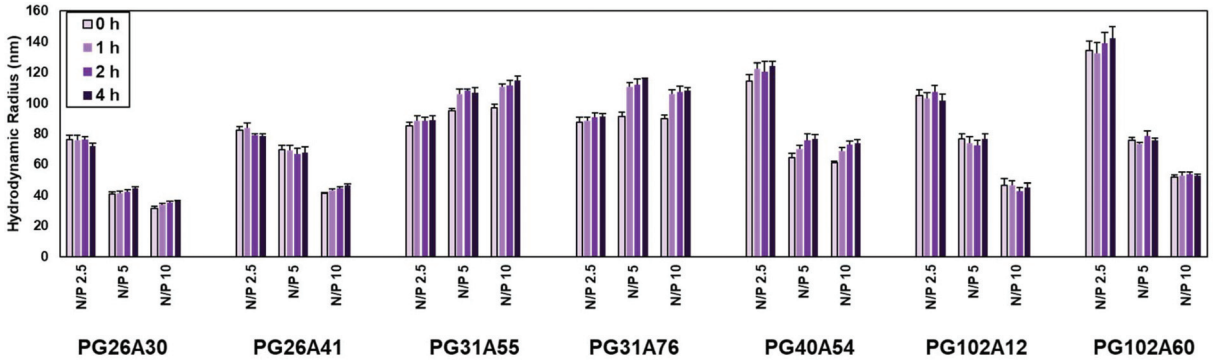

Fig. 3 Hydrodynamic radii of polyplexes as measured by dynamic light scattering (DLS). Polyplexes were formed by mixing equal volumes of pDNA and polymer solutions as N/P ratios of 2.5, 5, and 10. The polyplexes were incubated at room temperature for 1 h before diluting with OptiMEM. **PGxAy** polyplexes were measured at various time points (0 h, white bar; 1 h, diagonal stripes; 2 h, horizontal stripes, 4 h, black) after OptiMEM dilution.

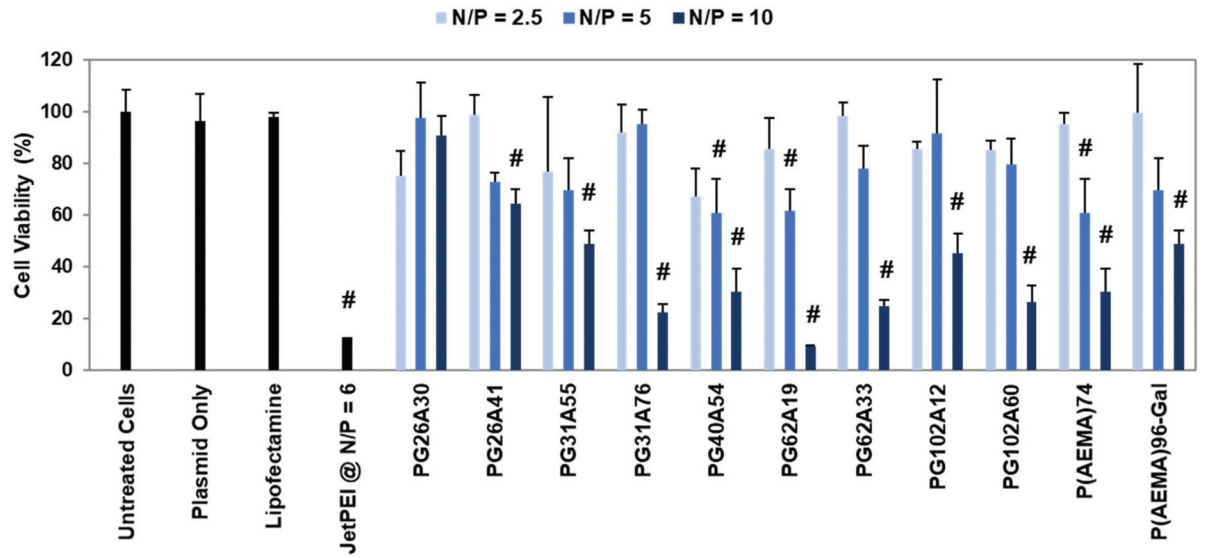

Fig. 4 HepG2 cell viability as determined by CCK-8 assay at various N/P ratios (2.5, light blue; 5, blue; 10, navy blue). Results were normalized to show 100% cell survival of untreated cells and presented as mean ± standard deviation (n = 3). Data analyzed by one-way ANOVA followed by a *post hoc* Tukey test. The '#' symbol indicates statistical difference compared to untreated cell control sample ($p < 0.05$).

fluorescent cyanine 5 (Cy5)-tag complexed to our polymer library. After 24 h, the percentage of Cy5-positive live cells were quantified by flow cytometry (Fig. S6†). ANOVA examination showed evidence that AEMA length and N/P ratio were not only the primary factors that influenced polyplex uptake, but the interaction term between these two variables were highly influential (Table S4†). Surprisingly, uptake does not seem to be sensitive to GalNAc length (Table S4†). Most polymers showed extensive internalization (83–99% Cy5 positive) compared to the commercial transfection reagent lipofectamine (72% Cy5 positive) and similar internalization to JetPEI (Fig. S6†). The **PG62A19** and **PG62A33** showed a substantial drop in internalization when increasing the dose from an N/P of 2.5 to 5 and 10. It should be noted the HepG2 cells transfected with these specific polyplexes exhibited low cell counts when analyzed by flow cytometry and it should be noted that these samples were from a previous synthesized batch used to directly compare the current polymer set to our previous study and we had limited sample availability.[10] Interestingly, the polyplexes formed without a GalNAc block ($PAEMA_{74}$ and $PAEMA_{96}$-Gal) showed nearly equivalent internalization to the diblock polymers. This could suggest alternative internalization pathways can lead to polyplex internalization, rather than just receptor-mediated endocytosis.

The transfection efficiency of each polymer in the library was examined *via* quantification of luciferase reporter gene expression from each dosed polyplex at the given N/P ratios (Fig. 5B). Briefly, HepG2 cells were transfected with the polyplexes formulated with a pCAG-FLuc plasmid (provided by Limelight Bio, Philadelphia, PA) at N/P ratios of 2.5, 5, and 10

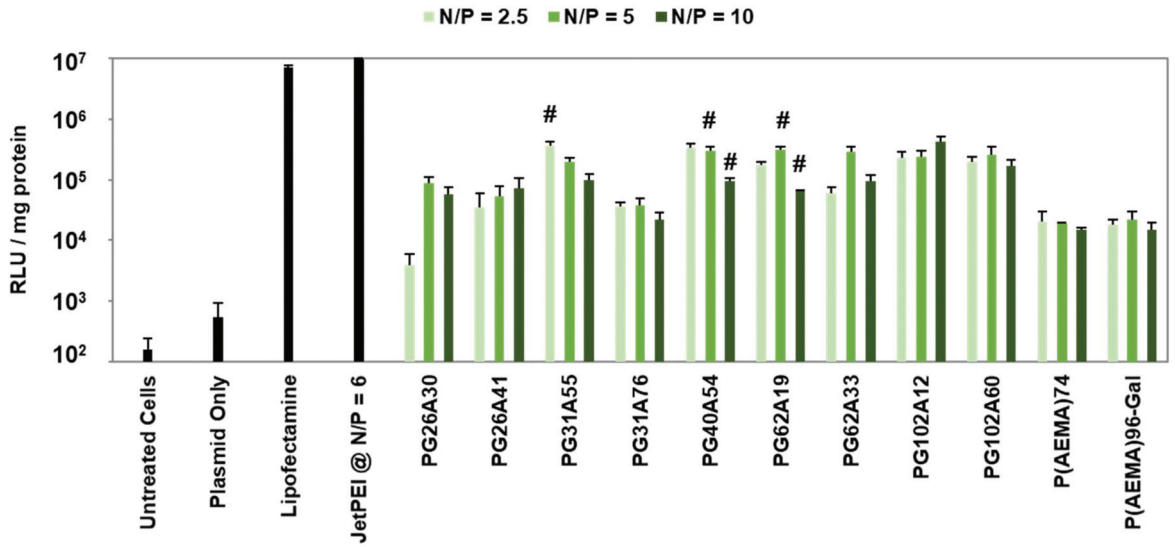

Fig. 5 Luciferase activity in HepG2 cells of polymer library at various N/P ratios (2.5, light green; 5, green; 10, dark green). The luciferase assay was performed 48 h post-transfection. Relative light units (RLU) per milligram of protein (RLU per mg protein) are reported as mean ± standard deviation (n = 3). Data analyzed by one-way ANOVA followed by pairwise t test with Bonferroni adjusted p-values. The '#' symbol indicates the differential in transfection performance between the highlighted formulation and the $P(AEMA)_{74}$ at the corresponding N/P ratio was statistically significant (FWER = 0.05).

then analyzed *via* the luciferase reporter assay kit (Promega, Madison, WI) 48 h post-transfection. Included in this study were the previously synthesized GalNAc-containing polymers **PG62A19** and **PG62A33** for direct comparison to the newly synthesized analogues.[10] All polymers showed an ability to elicit luciferase expression. Fascinatingly, for the diblock polymers, the GalNAc length of the polymer shows significant influence over the transfection efficiency, with longer GalNAc blocks eliciting a higher luciferase activity readout (Fig. 5, Table S5†). The lone exception is **P26A30**, where at N/P 2.5, the transfection efficiency drops about tenfold from N/P 5 or 10. Notably, the biggest difference in transfection efficiency – about tenfold – can be observed when comparing the luminescence of the **P31A76** to the **P102A19** diblock polymers at all N/P doses. The improved efficiency of **P102A19** over **P31A76** can be due to the composition length of each block: the MAGalNAc : AEMA block length for **P31A76** is 0.8 whereas the MAGalNAc : AEMA block length for **P102A19** is 17.2, which is the largest disparity in block length ratio for the entire library. Thus, this work shows that the overall GalNAc abundance in the polyplex can play a role in transfection efficiency, but only by greatly increasing the GalNAc block length are any efficacious affects apparent. The remainder of the library exhibits statistically similar variations on this theme for the diblock polymers. Interestingly, both the $PAEMA_{74}$ and $PAEMA_{96}$-Gal cationic homopolymers showed an ability to transfect HepG2 cells, albeit with about tenfold less efficacy (Fig. 5). Since $PAEMA_{96}$-Gal is composed of only 1.4 wt% GalNAc, the lack of improved transfection efficiency is unsurprising as the GalNAc end-group could be buried in the greater structure of the polyplex. Compare these data to a previous report from the Narain group, where PAEMA homopolymers consisting of 90 repeat units showed transfection efficiencies between 30–40%.[30] This work also shows that incorporation of a single GalNAc targeting moiety into the polymer ends did not adversely affect the ability for these polymers to transfect HepG2 cells, however, it is clearly not as effective as the multivalent block architectures. Multivalency is indeed important for improved transgene expression in this important cell type but not necessarily as important for internalization.

All data was also evaluated using analysis of variance (ANOVA), a statistical inference tool that identifies the most significant causes of variation in a dataset where multiple experimental factors are varied. To understand the relative contributions of these three variables (N/P ratio, GalNAc and AEMA block lengths), ANOVA was performed on the toxicity, luciferase, and Cy5-plasmid internalization datasets. At a given N/P ratio, AEMA block length was the primary determinant of polyplex uptake ($p < 10^{-4}$) with longer AEMA lengths being associated with lower intensities of Cy5 (Table S3†); conversely, uptake does not appear to be particularly sensitive to GalNAc length. In contrast, the ANOVA analysis for transfection presents a completely different picture, with GalNAc length identified as the clearly dominant factor (Table S4†). Polymers with longer GalNAc blocks resulted in higher luciferase expression (Fig. 5, Table S5†). The N/P ratio, however, only marginally influences luciferase expression, a finding that contrasts with the strong effect of N/P ratio on uptake. Cellular toxicity was a non-monotonic function of GalNac block length, with moderate/medium block lengths exhibiting higher levels of toxicity than short and long GalNac blocks (Table S6†).

Conclusion

In this work, we reported the synthesis of monomer **3** *via* a newly improved two-step, high-yielding route and a novel CTA

bearing a GalNAc end-group functionality. From this new route to **3**, we were then able to synthesize a suite of diblock copolymers containing a GalNAc block of varying lengths and a mono-functional GalNAc AEMA homopolymer. Each of these polymers were then evaluated for their colloidal stability and ability to bind DNA, as well as the corresponding polyplexes were evaluated for their cytotoxicity and transfection efficiency towards HepG2 cells. At higher N/P doses, most polymers showed increased toxicity as evident by the CCK-8 viability assays. All polymers showed an ability to transfect HepG2 cells at every N/P ratio tested. Multivariant ANOVA showed that the longer the GalNAc block length, the higher the luciferase activity (Tables S4–S6†). GalNAc length also was shown through this analysis to influence the transfection efficiency in tandem with AEMA block length and N/P ratios; by increasing the AEMA block length, the luciferase expression will depend on the GalNAc block length. The largest notable difference in transfection efficiency for the diblock polymers was **P31A76** and **P102A12**, where the MAGalNAc : AEMA ratio seem to play a moderate effect. Interestingly, both the $PAEMA_{74}$ and $PAEMA_{96}$-Gal cationic homopolymers showed nearly equivalent transfection efficacy. Incorporating a single GalNAc onto a cationic homopolymer did not seem to improve transfection efficiency, due to the potential burying of the targeting group within the polyplex. This study offers a more comprehensive study of the delivery capabilities of GalNAc diblock polymers, as well as expanding the chemical diversity of GalNAc-containing polymers, which is important for the expanding field of liver-targeted gene delivery.

Conflicts of interest

There are no conflicts to declare.

Acknowledgements

We would like to thank Limelight Bio for financial support of this project. We also thank Professor Timothy Lodge at the University of Minnesota for use of his refractometer. We also gratefully acknowledge Craig Van Bruggen for helpful discussions and Joseph K. Hexum for help on figure design.

References

1 V. Sudhakar and R. M. Richardson, *Neurotherapeutics*, 2019, **16**, 166–175.
2 F. Touzot, D. Moshous, R. Creidy, B. Neven, P. Frange, G. Cros, L. Caccavelli, J. Blondeau, A. Magnani, J. M. Luby, B. Ternaux, C. Picard, S. Blanche, A. Fischer, S. Hacein-Bey-Abina and M. Cavazzana, *Blood*, 2015, **125**, 3563–3569.
3 B. Greenberg, A. Yaroshinsky, K. M. Zsebo, J. Butler, G. M. Felker, A. A. Voors, J. J. Rudy, K. Wagner and R. J. Hajjar, *JACC Heart Fail.*, 2014, **2**, 84–92.
4 D. Cross and J. K. Burmester, *Clin. Med. Res.*, 2006, **4**, 218–227.
5 N. Nayerossadat, T. Maedeh and P. A. Ali, *Adv. Biomed. Res.*, 2012, **1**, 27.
6 M. Foldvari, D. W. Chen, N. Nafissi, D. Calderon, L. Narsineni and A. Rafiee, *J. Controlled Release*, 2016, **240**, 165–190.
7 M. Ramamoorth and A. Narvekar, *J. Clin. Diagn. Res.*, 2015, **9**, GE01.
8 D. Fischer, T. Bieber, Y. Li, H. P. Elsässer and T. Kissel, *Pharm. Res.*, 1999, **16**, 1273–1279.
9 P. Van De Wetering, J. Y. Cherng, H. Talsma and W. E. Hennink, *J. Controlled Release*, 1997, **49**, 59–69.
10 Y. K. Dhande, B. S. Wagh, B. C. Hall, D. Sprouse, P. B. Hackett and T. M. Reineke, *Biomacromolecules*, 2016, **17**, 830–840.
11 Y. Wu, M. Wang, D. Sprouse, A. E. Smith and T. M. Reineke, *Biomacromolecules*, 2014, **15**, 1716–1726.
12 N. P. Ingle, L. Xue and T. M. Reineke, *Mol. Pharm.*, 2013, **10**, 4120–4135.
13 K. von Gersdorff, N. N. Sanders, R. Vandenbroucke, S. C. De Smedt, E. Wagner and M. Ogris, *Mol. Ther.*, 2006, **14**, 745–753.
14 J. Rejman, M. Conese and D. Hoekstra, *J. Liposome Res.*, 2006, **16**, 237–247.
15 T. H. Nguyen and N. Ferry, *Gene Ther.*, 2004, **11**, S76–S84.
16 R. N. Aravalli, J. D. Belcher and C. J. Steer, *Liver Transplant.*, 2015, **21**, 718–737.
17 T. C. Gust and M. Zenke, *Sci. World J.*, 2002, **2**, 224–229.
18 Z. Tan, Y. K. Dhande and T. M. Reineke, *Bioconjugate Chem.*, 2017, **28**, 2985–2997.
19 R. Rouet, B. A. Thuma, M. D. Roy, N. G. Lintner, D. M. Rubitski, J. E. Finley, H. M. Wisniewska, R. Mendonsa, A. Hirsh, L. De Oñate, J. Compte Barrón, T. J. McLellan, J. Bellenger, X. Feng, A. Varghese, B. A. Chrunyk, K. Borzilleri, K. D. Hesp, K. Zhou, N. Ma, M. Tu, R. Dullea, K. F. McClure, R. C. Wilson, S. Liras, V. Mascitti, J. A. Doudna, L. de Onate, J. Compte Barron, T. J. McLellan, J. Bellenger, X. Feng, A. Varghese, B. A. Chrunyk, K. Borzilleri, K. D. Hesp, K. Zhou, N. Ma, M. Tu, R. Dullea, K. F. McClure, R. C. Wilson, S. Liras, V. Mascitti and J. A. Doudna, *J. Am. Chem. Soc.*, 2018, **140**, 6596–6603.
20 J. K. Nair, J. L. S. Willoughby, A. Chan, K. Charisse, M. R. Alam, Q. Wang, M. Hoekstra, P. Kandasamy, A. V. Kelin, S. Milstein, N. Taneja, J. Oshea, S. Shaikh, L. Zhang, R. J. Van Der Sluis, M. E. Jung, A. Akinc, R. Hutabarat, S. Kuchimanchi, K. Fitzgerald, T. Zimmermann, T. J. C. Van Berkel, M. A. Maier, K. G. Rajeev and M. Manoharan, *J. Am. Chem. Soc.*, 2014, **136**, 16958–16961.
21 A. D. Springer and S. F. Dowdy, *Nucleic Acid Ther.*, 2018, **28**, 109–118.
22 H. X. Wang, M. H. Xiong, Y. C. Wang, J. Zhu and J. Wang, *J. Controlled Release*, 2013, **166**, 106–114.

23 O. Khorev, D. Stokmaier, O. Schwardt, B. Cutting and B. Ernst, *Bioorg. Med. Chem.*, 2008, **16**, 5216–5231.
24 Y. Wang, R. Z. Yu, S. Henry and R. S. Geary, *Expert Opin. Drug Metab. Toxicol.*, 2019, **15**, 475–485.
25 H. J. M. Hempen, J. de Lange, A. Langendoen, C. Hoes, J. H. van Boom, H. H. Spanjer and T. J. C. Van Berkel, *J. Med. Chem.*, 1984, **27**, 1306–1312.
26 P. C. N. Rensen, S. H. Van Leeuwen, L. A. J. M. Sliedregt, T. J. C. Van Berkel and E. A. L. Biessen, *J. Med. Chem.*, 2004, **47**, 5798–5808.
27 R. T. Lee and Y. C. Lee, *Bioconjugate Chem.*, 1997, **8**, 762–765.
28 T. P. Prakash, W. Brad Wan, A. Low, J. Yu, A. E. Chappell, H. Gaus, G. A. Kinberger, M. E. Østergaard, M. T. Migawa, E. E. Swayze and P. P. Seth, *Bioorg. Med. Chem. Lett.*, 2015, **25**, 4127–4130.
29 M. T. Migawa, T. P. Prakash, G. Vasquez, W. B. Wan, J. Yu, G. A. Kinberger, M. E. Stergaard, E. E. Swayze and P. P. Seth, *Bioorg. Med. Chem. Lett.*, 2016, **26**, 2194–2197.
30 B. Thapa, P. Kumar, H. Zeng and R. Narain, *Biomacromolecules*, 2015, **16**, 3008–3020.
31 D. Sprouse and T. M. Reineke, *Biomacromolecules*, 2014, **15**, 2616–2628.
32 H. R. Phillips, Z. P. Tolstyka, B. C. Hall, J. K. Hexum, P. B. Hackett and T. M. Reineke, *Biomacromolecules*, 2019, **20**, 1530–1544.
33 E. Xu, A. E. Smith, S. E. Kirkland and C. L. McCormick, *Macromolecules*, 2008, **41**, 8429–8435.
34 D. J. Keddie, G. Moad, E. Rizzardo and S. H. Thang, *Macromolecules*, 2012, **45**, 5321–5342.
35 J. A. Hubbell, D. S. Wilson, K. Brünggel and K. M. Lorentz, WO/2019/217628, 2019.